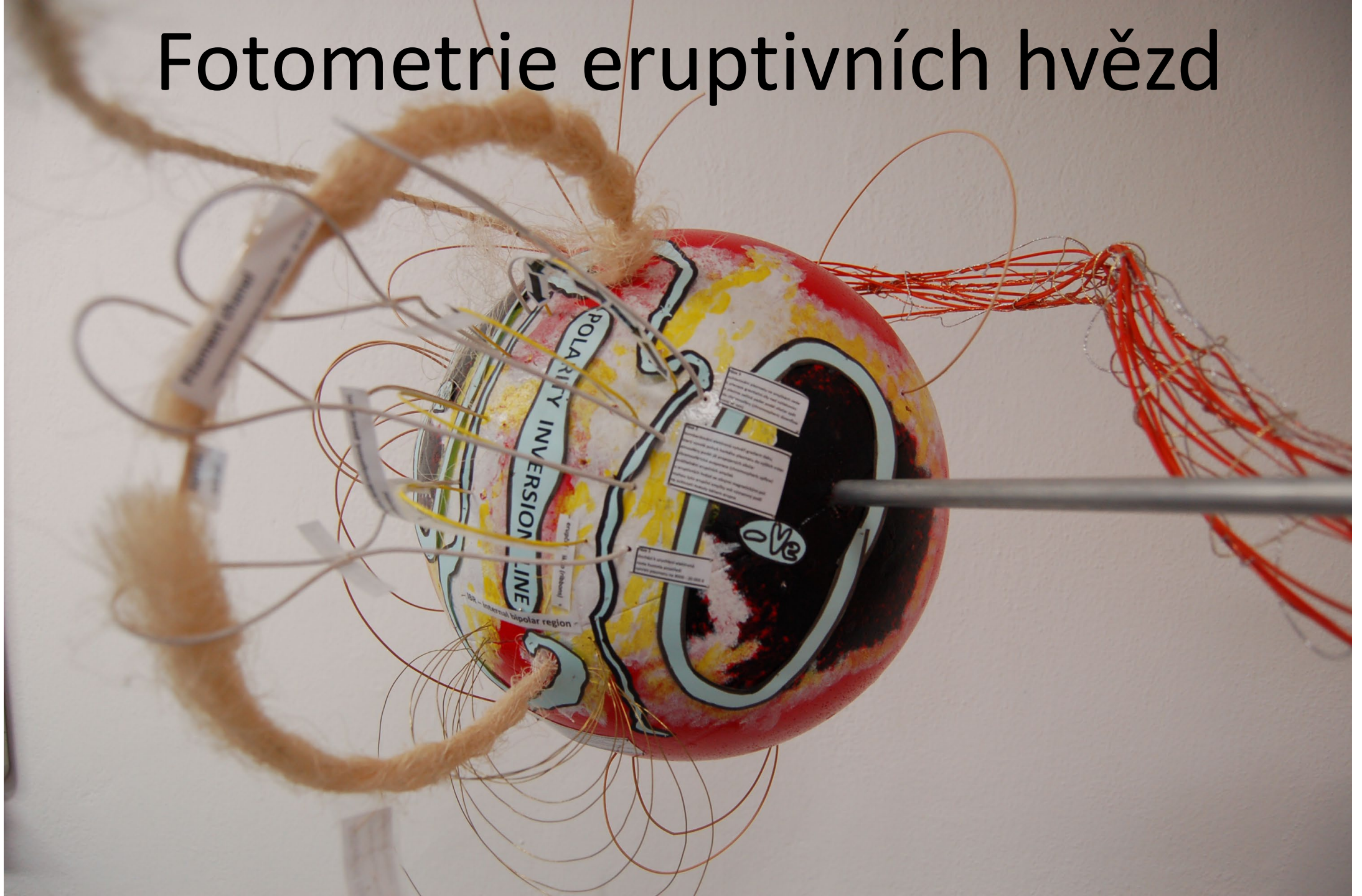
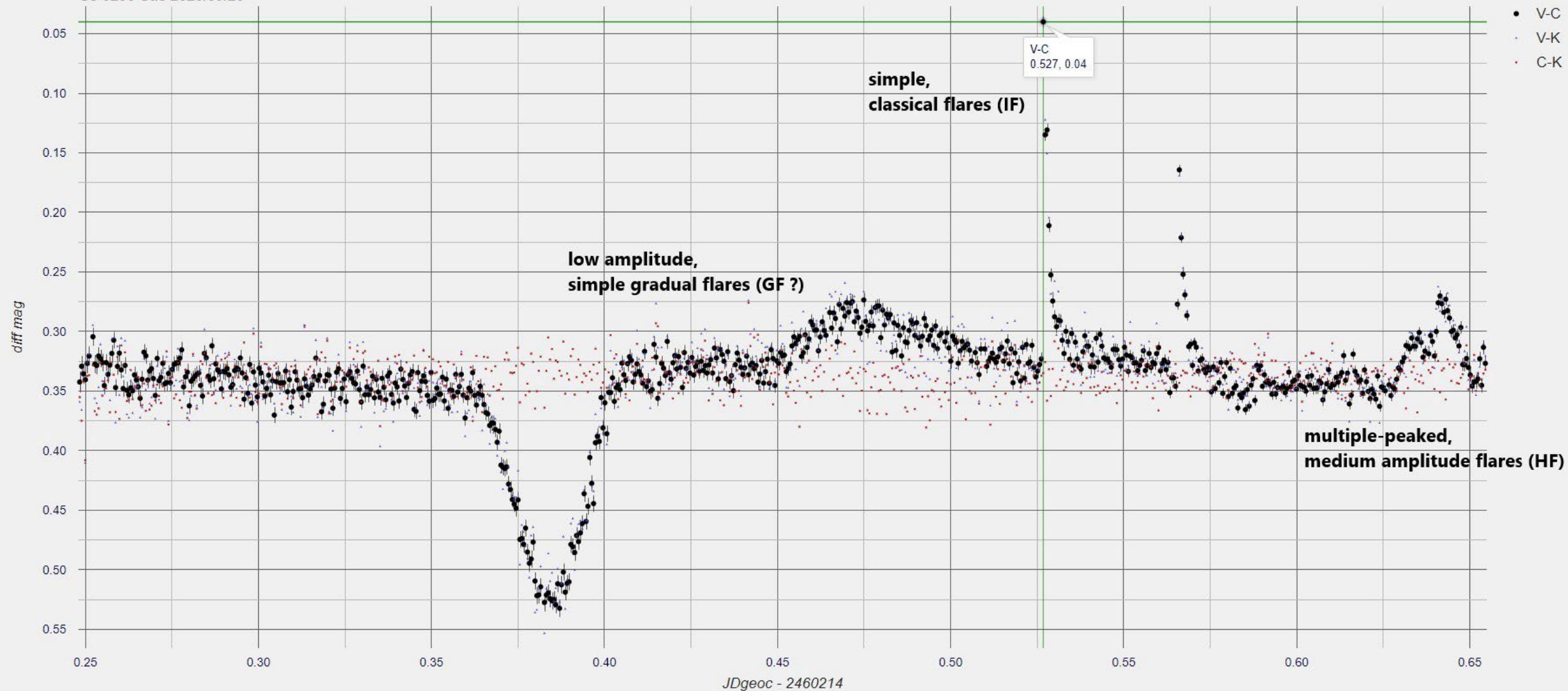


Fotometrie eruptivních hvězd



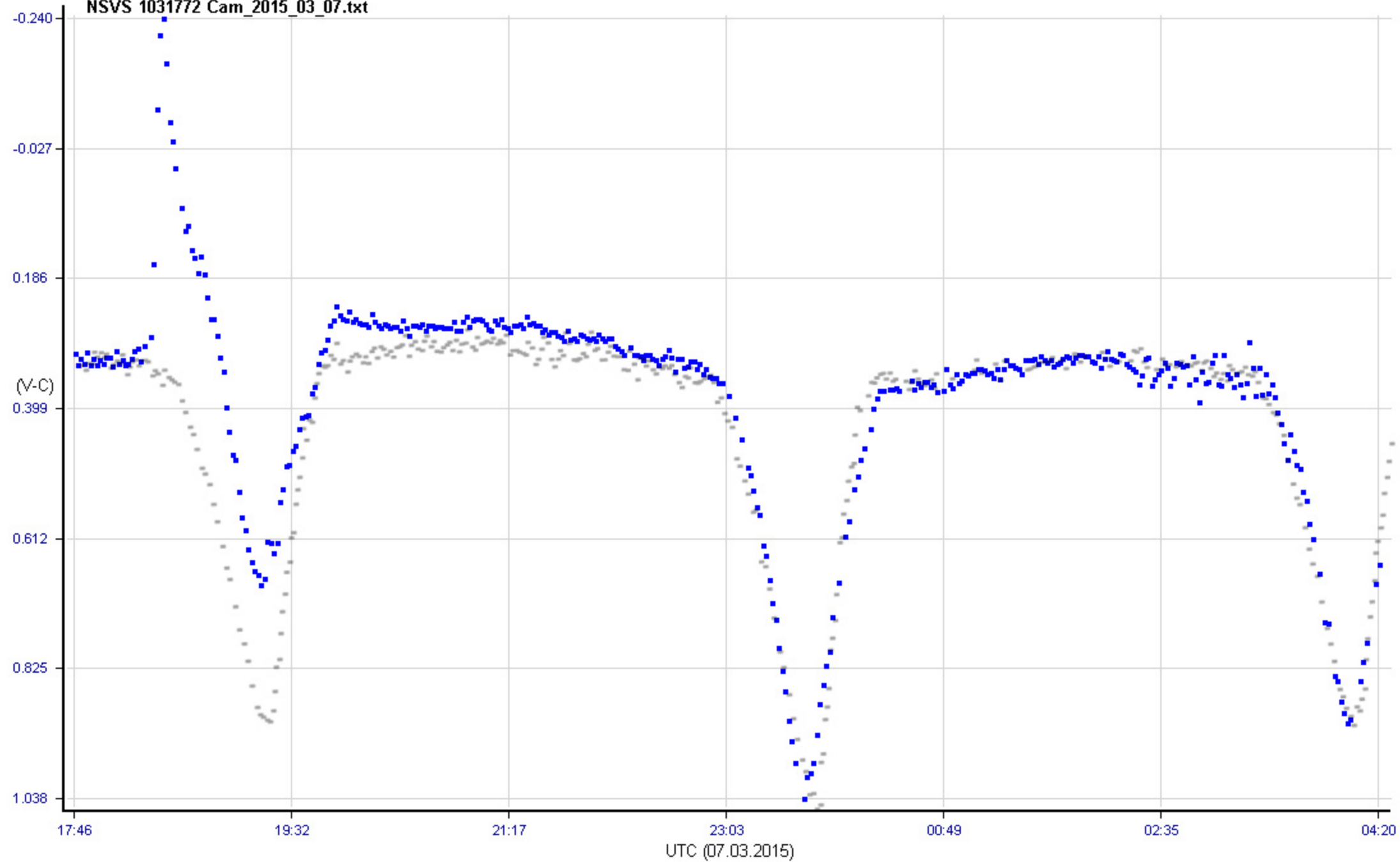
GJ 3236 Cas 2023/09/26



all data V-C V-C & V-K V-C & C-K V-K V-K & C-K C-K view finding chart size1: 4 size2: 1 V-C: V-K: C-K: error bars width: 1 (0 = no error bars); chart is zoomable (right click to reset zoom)

- Primary minimum: JDgeoc: -; JDhel: - (error: -)
- Secondary minimum: JDgeoc: 2460214.38403; JDhel: 2460214.38546 (error: 0.00015)
- Measurements: 736x45sec

NSVS 1031772 Cam_2015_03_07.txt



JOURNAL ARTICLE

Multiwavelength observation of an active M-dwarf star EV Lacertae and its stellar flare accompanied by a delayed prominence eruption

Get access >

Shun Inoue ✉, Teruaki Enoto, Kosuke Namekata, Yuta Notsu, Satoshi Honda, Hiroyuki Maehara, Jiale Zhang, Hong-Peng Lu, Hiroyuki Uchida, Takeshi Go Tsuru ...
[Show more](#)

Publications of the Astronomical Society of Japan, Volume 76, Issue 2, April 2024, Pages 175–190, <https://doi.org/10.1093/pasj/psae001>

Published: 29 January 2024 **Article history** ▼

Abstract

We conducted four-night multiwavelength observations of an active M-dwarf star EV Lacertae on 2022 October 24–27 with simultaneous coverage of soft X-rays (NICER; 0.2–12 keV, Swift XRT; 0.2–10 keV), near-ultraviolet (Swift UVOT/UVW2; 1600–3500 Å), optical photometry (TESS; 6000–10000 Å), and optical spectroscopy (Nayuta/MALLS; 6350–6800 Å). During the campaign, we detected a flare starting at 12:28 UTC on October 25 with a white-light bolometric energy of 3.4×10^{32} erg. At about 1 h after this flare peak, our H α spectrum showed a blueshifted excess component at a corresponding velocity of $\sim 100 \text{ km s}^{-1}$. This may indicate that the prominence erupted with a 1 h delay of the flare peak. Furthermore, the simultaneous 20 s cadence near-ultraviolet (NUV) and white-light curves show gradual and rapid brightening behaviors during the rising phase at this flare. The ratio of flux in NUV to white light at the gradual brightening was ~ 0.49 , which may suggest that the temperature of the blackbody is low ($< 9000 \text{ K}$) or the maximum energy flux of a non-thermal electron beam is less than $5 \times 10^{11} \text{ erg cm}^{-2} \text{ s}^{-1}$. Our simultaneous observations of the NUV and white-light flare raise the issue of a simple estimation of UV flux from optical continuum data by using a blackbody model.

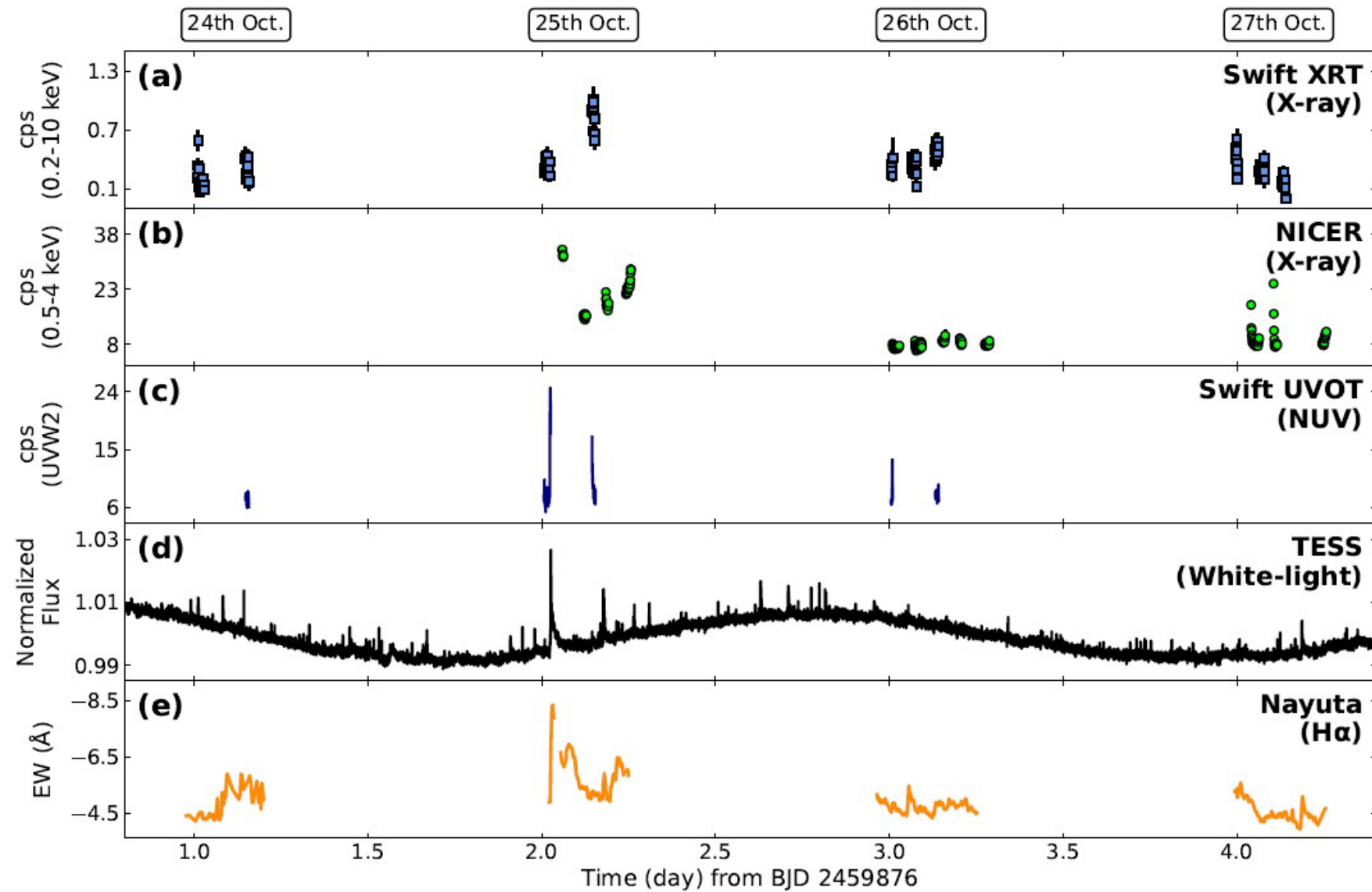


Fig. 1. Four-days light curves of EV Lac during our observation campaign on 2022 October 24–27. The time-zero of 2459876 BJD corresponds to 2022 October 23 11:53 UTC. (a) Swift XRT count rates (counts s^{-1}) in 0.2–10 keV. The time bin and error bars are 64 seconds and one standard deviation statistical error, respectively. (b) NICER count rates (counts s^{-1}) in 0.5–4 keV. The time bin and error bars are 64 seconds and one standard deviation statistical error, respectively. (c) Swift UVOT count rates (counts s^{-1}) in the UVW2 band (1600–3500 Å). The time bin is 20 seconds. (d) TESS white-light light curve shown at 6000–10000 Å. The flux is normalized by the median value. The time bin is 20 seconds. (e) Nayuta H α -line light curve. The equivalent width (Å) is negative values for the emission line flux in this light curve. The time bin is 180 seconds except for during the part of October 24.

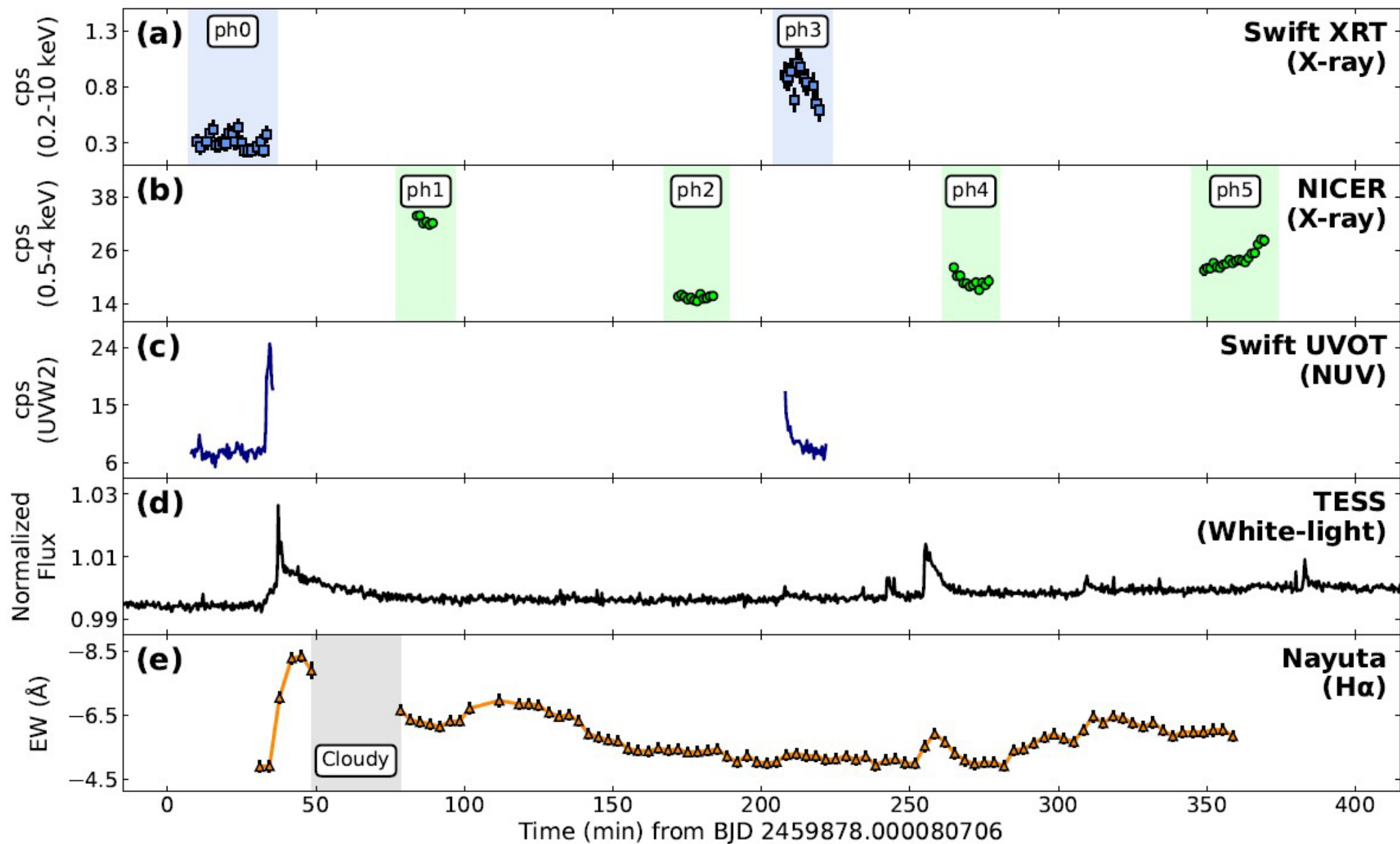


Fig. 2. Enlarged light curves of EV Lac on 2022 October 25. The time-zero of 2459878.000080706 BJD corresponds to 2022 October 25 11:52 UTC. Phase numbers in our X-ray spectral analysis are shown as “ph *” in panel (a) and (b). The gray zone in panel (e) is cloudy time.

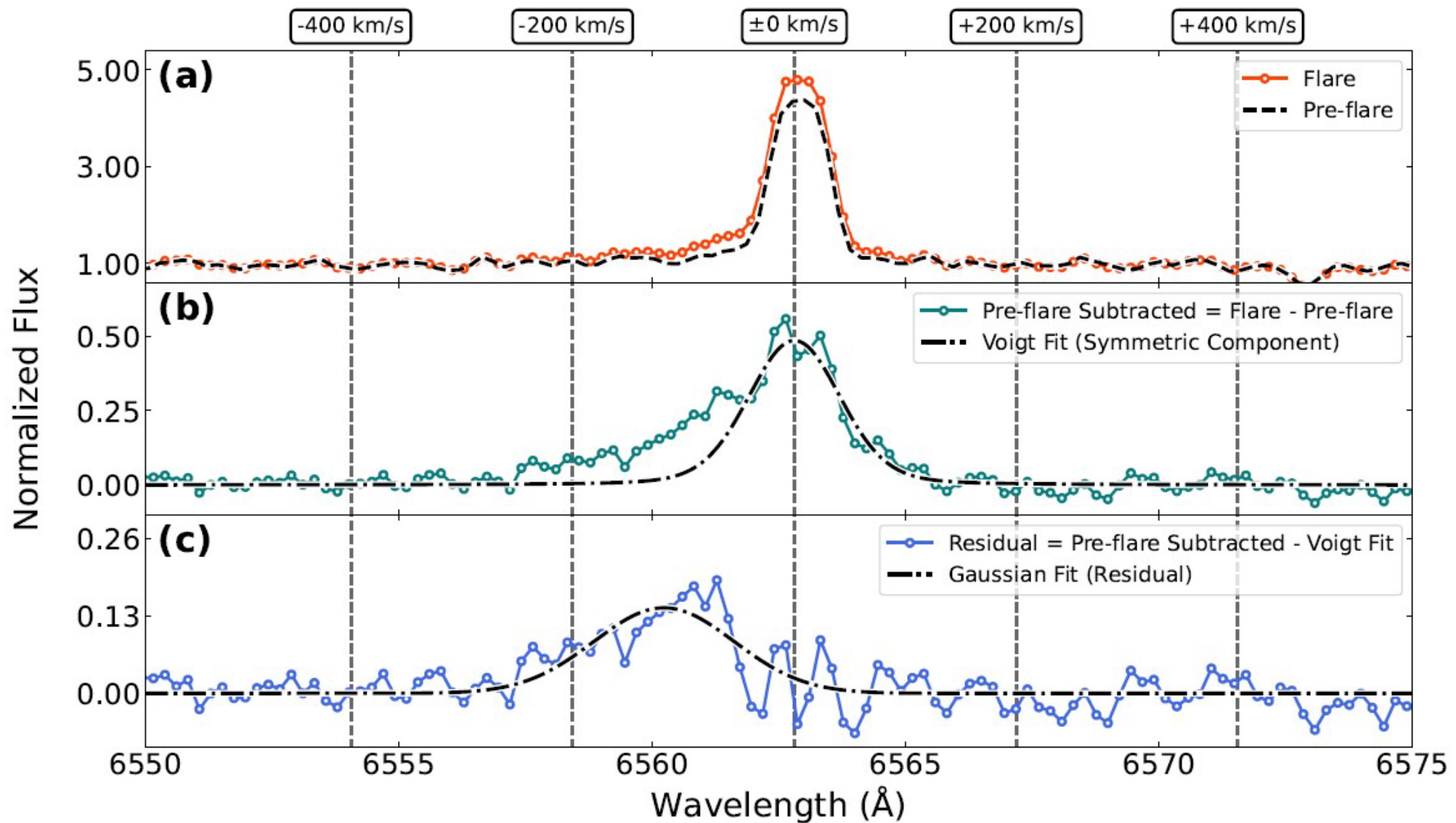


Fig. 3. An example of normalized H α spectra extracted from the time period of 127–129 min in the light curve of Figure 2. Gray vertical dashed lines show Doppler velocity from the line center at 6562.8 \AA . (a) Comparison of the continuum at the 127–129 min range (orange solid line) with that in the pre-flare data at the 30–35 min (black dashed line). (b) Pre-flare subtracted spectrum of panel (a). The black dashdot line represents the Voigt function fitting only used for the red side of the line center (6562.8–6600 \AA). (c) Residual between the pre-flare subtracted spectrum (panel b) and the best-fit Voigt function result in panel (b). The black dashdot line represents the Gaussian fitting.

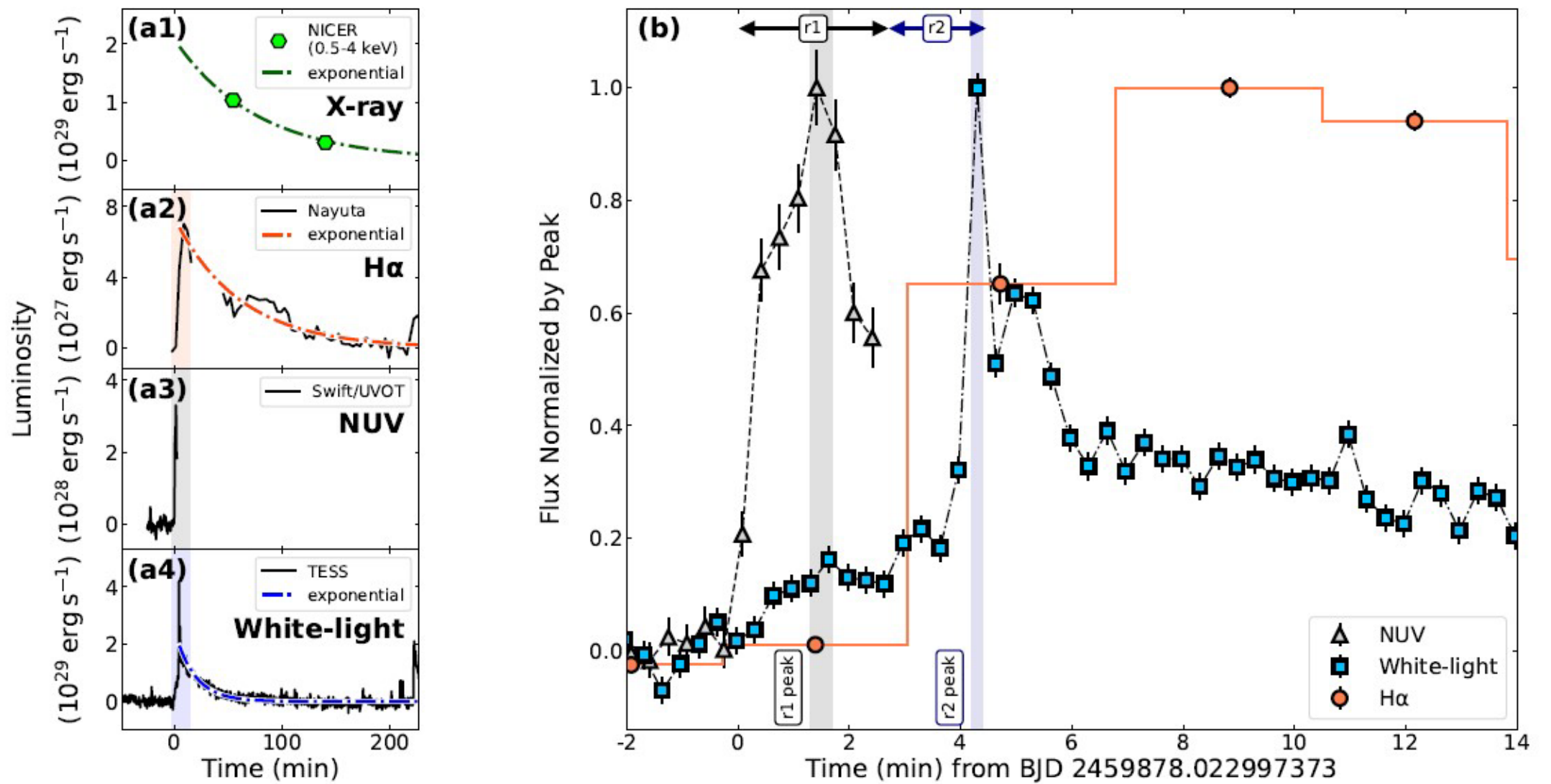


Fig. 8. (a1-a4) Quiescent-subtracted light curves. The time zero point is set to the beginning of the flare. The dashdot lines show the exponential function fitted for the decay phase of the light curve. (a1) Flare luminosity of 0.5–4 keV X-ray. (a2) Flare luminosity of H α . Note that the luminosity of the blue-shifted excess component is removed in this curve. (a3) Flare luminosity of UVW2 band (1600–3500 Å). (a4) Flare luminosity of white light (6000–10000 Å). (b) Enlarged light curves around the rising phase of the flare, which corresponds to the shaded time intervals in panel (a2–a4). All curves are normalized by their peak values. Aqua triangle, blue square, and orange circle represent NUV, white-light, and H α , respectively. Blue and green shaded regions indicate gradual and rapid phase of white-light, respectively.



